# Defect States at the $TiO_2(110)$ Surface Probed by Resonant Photoelectron Diffraction

P. Krüger,[1] S. Bourgeois,[1] B. Domenichini,[1] H. Magnan,[2] D. Chandesris,[3] P. Le Fèvre,[3] A. M. Flank,[3] J. Jupille,[4] L. Floreano,[5] A. Cossaro,[5] A. Verdini,[5] and A. Morgante[5,6]

[1]*Institut Carnot de Bourgogne, UMR 5209 CNRS-Université de Bourgogne, BP 47870, 21078 Dijon Cedex, France*
[2]*Service de Physique et Chimie des Surfaces et Interfaces, CEA Saclay, 91191 Gif-sur-Yvette, France*
[3]*Synchrotron SOLEIL, L'Orme des Merisiers, BP 48, 91192 Gif-sur-Yvette, France*
[4]*Institut des NanoSciences de Paris, CNRS, Campus Boucicaut, 140 rue de Lourmel, 75015 Paris, France*
[5]*Laboratorio Nazionale TASC-INFM, Elettra Synchrotron Light Source, 34012 Basovizza-Trieste, Italy*
[6]*Dipartimento di Fisica, Università di Trieste, Via Valerio 2, 34127 Trieste, Italy*

(Received 30 May 2006; revised manuscript received 2 November 2007; published 4 February 2008)

The charge distribution of the defect states at the reduced $TiO_2(110)$ surface is studied via a new method, the resonant photoelectron diffraction. The diffraction pattern from the defect state, excited at the Ti-2*p*-3*d* resonance, is analyzed in the forward scattering approach and on the basis of multiple scattering calculations. The defect charge is found to be shared by several surface and subsurface Ti sites with the dominant contribution on a specific subsurface site in agreement with density functional theory calculations.

DOI: 10.1103/PhysRevLett.100.055501 PACS numbers: 68.35.Dv, 61.05.js

Defects play an important role in many chemical reactions at surfaces. The understanding of their structural and electronic properties is a major issue of surface chemistry. The rutile $TiO_2(110)$ surface is often considered as a model system for oxide surfaces and has been the subject of extensive studies [1]. Under standard preparation conditions for the $(1 \times 1)$ surface the major defect type in the near surface region is oxygen vacancies at the bridging (O1) site ("V" in Fig. 1) [1]. Each oxygen vacancy gives rise to two excess electrons and the appearance of new electronic states in the $TiO_2$ band gap at about 2 eV above the valence band maximum. These defect states are mainly of Ti-3*d* character as was shown by resonant photoemission experiments [2,3]. However, the distribution of the excess charge, the knowledge of which is crucial in modeling the $TiO_2(110)$ surface and its chemical and photochemical behavior, remains an open issue. First-principles studies devoted to the question are strongly conflicting since their conclusions depend on the approximation used for the exchange and correlation (XC) potential. Pure density functional theory (DFT) approaches generally describe the defect state as delocalized over several Ti sites in the surface and subsurface layer [4,5]. In contrast, calculations based on either Hartree-Fock or hybrid XC-functional approaches predict that all defect charge is found in the surface layer, the two excess electrons being localized on two specific surface Ti sites [6,7]. On the experimental side, there is some evidence that the excess electrons are unpaired and localized [8]. There is, however, no *experimental* answer to the question on *which* Ti sites the excess electrons are localized and this is because there has been, to date, no suggestion of any relevant experimental approach to unravel charge localization.

In this Letter, the distribution of excess electrons over the 3*d* orbitals of the surface and subsurface Ti atoms is directly probed by means of a novel technique, the resonant photoelectron diffraction (PED). The photoelectron diffraction is recorded for photoelectrons from the Ti-3*d* defect state which are resonantly excited at the Ti-2*p*-3*d* resonance. At this resonance, the defect state photoemission is strongly enhanced [3], which was crucial for obtaining a sufficient signal-to-noise ratio in PED. The experimental data are analyzed both in the forward scattering approach and through multiple scattering calculations.

The experiments were performed at the ALOISA beam line [9] of the Elettra Synchrotron Light Source in Trieste, Italy. The $TiO_2(110)$ single crystal was cleaned by 1 keV $Ar^+$ bombardment and annealed for 45 min at 870 K under ultrahigh vacuum. This standard protocol produces flat $(1 \times 1)$-terminated surfaces with a bridging oxygen vacancy concentration of a few percent [10]. The PED from the defect states was recorded for a photon energy at the maximum of the $L_2$-edge resonance (462 eV). The x-ray beam was impinging in grazing incidence and the light

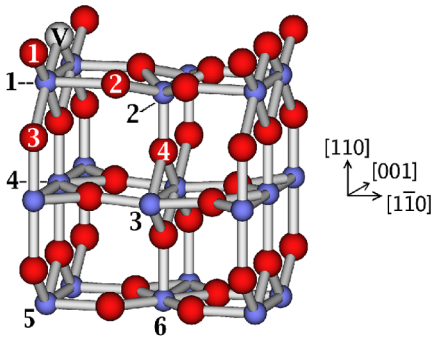


FIG. 1 (color online). Ball and stick model of the $TiO_2(110)$ surface. Big red (small blue) balls are O (Ti) atoms. V indicates a bridging oxygen (O1) vacancy.

 

polarization was normal to the surface. The angle resolved photoemission intensity $I(\theta, \phi)$ was measured for polar angles $\theta$ up to 80° and for azimuthal angles $\phi$ over a range of 150° including the two symmetry directions [001] and $[1\bar{1}0]$. The data were symmetrically repeated according to the $C2v$ point symmetry of the $TiO_2(110)$ surface. We consider the azimuthal anisotropy function $\chi(\theta, \phi) = [I(\theta, \phi)/I_0(\theta)] - 1$ where $I_0(\theta)$ is the average of $I(\theta, \phi)$ over $\phi \in (0, 360)$. A plot of $\chi$ over $(\theta, \phi)$ will be called a "PED pattern" in the following.

As a reference, we have first measured the nonresonant PED from the Ti-$2p_{3/2}$ core level taken with a photon energy of 920 eV so that the kinetic energy of the photoelectrons was nearly the same (460 eV) as in the case of the resonant PED from the defect state. The two PED patterns are shown in Fig. 2. Since PED probes the local environment around the emitting Ti atoms, the strong difference between the two patterns immediately indicates that the defect charge is not uniformly distributed over all Ti sites (as is the Ti-$2p$ charge). Indeed, the analysis of the PED is shown hereafter to provide quantitative information about the defect charge distribution.

The positions of all major diffraction peaks (bright spots) in Fig. 2 agree well with interatomic directions from Ti sites, as it can be expected from a forward scattering picture. This is shown in the lower panels of Fig. 2, where we have marked near-neighbor interatomic directions from surface and subsurface Ti atoms. The angles were calculated using the recent structural data in Ref. [11]. The good agreement for all bright spots of the Ti-$2p$ pattern, between peak positions and interatomic directions (<5°), validates the forward scattering picture for the kinetic energy of 460 eV used here. For the defect state PED, the peak positions nicely match the interatomic directions Ti1-O1, Ti3-Ti2, and/or Ti4-Ti1, as well as Ti3-O2. The spots close to the Ti2-O2 and Ti2-O1 directions are very diffuse and so their assignments are tentative. Note that without a strong surface relaxation involving the Ti2 and O2 atoms [12], the Ti2-O2 direction would be parallel to the surface and could not be observed.

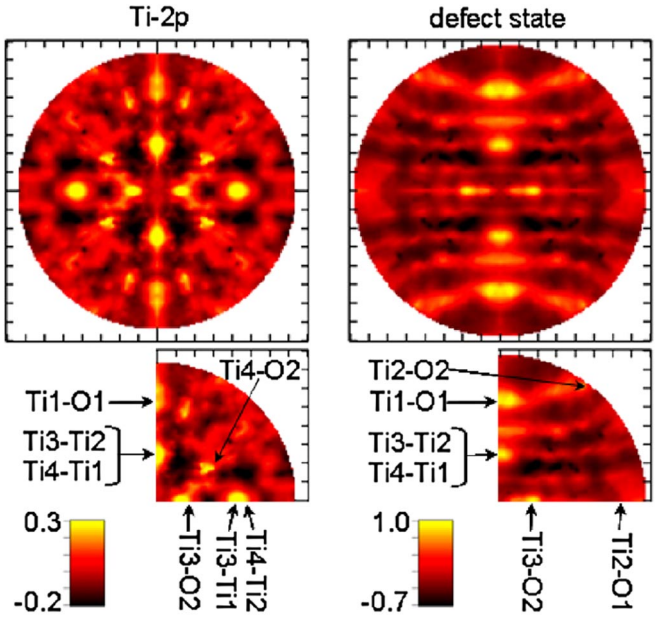


FIG. 2 (color online). Experimental photoelectron diffraction (PED) patterns $\chi(\theta, \phi)$. Left: Standard PED from the Ti-$2p_{3/2}$ core level. Right: Resonant PED from the defect state. The projection is linear in $\theta$ with the surface normal ($\theta = 0$) in the center. Ticks are drawn at every 10°. $\phi = 0$ ($\phi = 90$) is found at 3 o'clock (12 o'clock) and corresponds to the $[1\bar{1}0]$ ([001]) direction.

From these assignments, qualitative conclusions can be drawn about the defect state charge distribution. The observation of a scattering peak Ti($n$)-$X$ implies the existence of photoemission from atom Ti($n$). For the defect state PED this means that atom Ti($n$) must carry some defect state charge. The observation of peaks Ti1-O1, Ti2-O1, Ti2-O2, and Ti3-O2 then shows that substantial fractions of the total defect state charge are located on sites Ti1, Ti2, and Ti3. The absence of the Ti4-O2 peak in the defect state PED compared to its brightness in the Ti-$2p$ PED suggests that the amount of defect charge on site Ti4 is negligible.

In order to quantitatively analyze the experimental data, multiple scattering calculations were performed using the PED program package MSCD [13]. The $TiO_2(110)$ surface was modeled with a semielliptical cluster containing 178 atoms and one O1 vacancy at the center of the surface layer. Again the structural data of Ref. [11] were used. The multiple scattering series summed up to the fifth order was found sufficiently converged by comparison with eighth order calculations. The dipole matrix elements and the phase shifts were obtained from a self-consistent band structure calculation of bulk $TiO_2$ using the linear muffin-tin orbital (LMTO) method [14]. Since currently no computational methods are available for PED that can take account of the resonant photoemission (RP) process, we have approximated it by calculating the direct photoemission (DP) from localized Ti-$3d$ orbitals and averaged over all magnetic quantum numbers $m_l$. This approximation can be expected to be a very good one for two reasons. First, the emitted waves in DP and RP are the same, except for a possible, small difference of the angular momenta [15]. Second, at high kinetic energy, the PED pattern is known to be dominated by scattering effects and the angular momentum character of the emitted wave is of minor importance, as we have also checked by test calculations.

We have calculated the PED for emission from the six inequivalent Ti sites on the first three TiO layers, labeled Ti(1)–Ti(6) (see Fig. 1). Among the different Ti($n$) sites in the cluster, the emitter was taken to be the one closest to the O1 vacancy. The calculated PED patterns are shown in Fig. 3. For the emitters Ti1 and Ti2, the brightest spots are found at near-neighor directions (Ti1-O1 and Ti2-O1, Ti2-

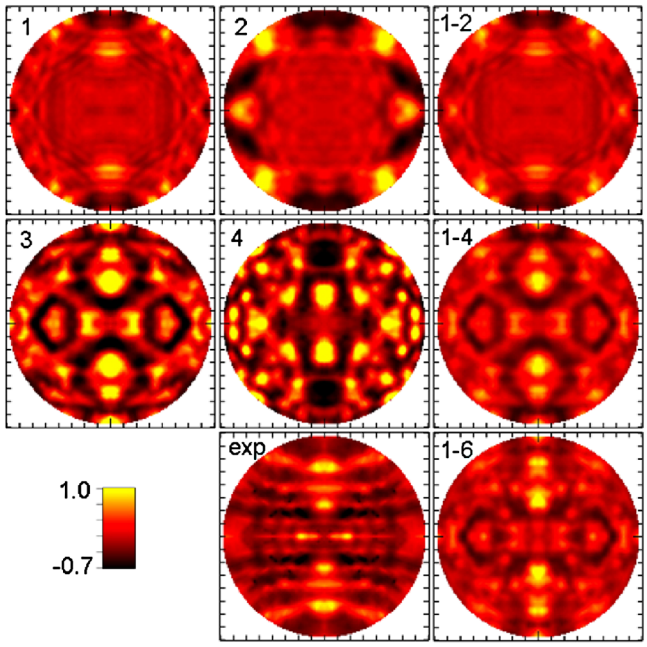


FIG. 3 (color online). Calculated photoelectron diffraction patterns from the defect level along with the experimental one ("exp"). Pattern "$n$" ($n = 1, \ldots, 4$) corresponds to emission from atom Ti($n$) alone. Pattern "1–$n$" corresponds to a weighted sum over the emission intensities of Ti(1) to Ti($n$), with relative weights as given in Table I and obtained through $R$-factor minimization.

O2, respectively, see Fig. 2) in agreement with the forward scattering approach. The calculated patterns from the subsurface emitters, Ti3 and Ti4, are much more complex and go beyond the forward scattering picture. The peak assignments in Fig. 2 for Ti3 and Ti4 are nevertheless essentially confirmed.

In order to determine the defect state charge distribution, a theoretical anisotropy function $\chi_t$ has been fitted to the experimental one $\chi_e$. For the theoretical photoemission intensity $I_t$ a weighted sum over several Ti sites has been taken: $I_t = \sum_n w_n I_n$, where $I_n$ is the photoemission intensity for the single emitter Ti($n$) and $w_n$ is its relative weight. The $w_n$ were determined by minimizing the following reliability ($R$) factor: $R = \int(\chi_e - \chi_t)^2 d\Omega / \int(\chi_e^2 + \chi_t^2) d\Omega$, where $\Omega = (\theta, \phi)$ is the solid angle and the $\theta$ integration was done from 0° to 78°. The results of the $R$-factor analysis are shown in Table I. Let us first note that the strong inhomogeneity of the weight distributions $\{w_n\}$ in Table I is highly significant. Equal weight for all six Ti sites would lead to $R = 0.586$, which is much larger than the minimum value $R = 0.477$. This is in contrast to the Ti-2$p$ PED, for which much more homogeneous weights (between 0.10 and 0.26) were found with the same computational method. In that case, the minimum $R$ factor (0.572) is not significantly lower than the $R$ value (0.586) obtained for equal weight on all six Ti atoms.

TABLE I. Results of $R$-factor analysis for the defect state PED pattern. $R_n$ is the $R$ factor for emission from site Ti($n$) alone. Model 1–$n$ means that atoms Ti1, …, Ti($n$) were included in the $R$-factor minimization.

| Site | Ti1 | Ti2 | Ti3 | Ti4 | Ti5 | Ti6 | |
|---|---|---|---|---|---|---|---|
| $R_n$ | 0.789 | 0.855 | 0.644 | 1.017 | 0.758 | 0.781 | |
| Model | Relative weights $w_n$ | | | | | | $R$ |
| 1–2 | 0.75 | 0.25 | | | | | 0.774 |
| 1–4 | 0.14 | 0.20 | 0.65 | 0.01 | | | 0.552 |
| 1–6 | 0.08 | 0.11 | 0.34 | 0.00 | 0.27 | 0.20 | 0.477 |

The contributions of the different Ti atoms to the PED pattern are now considered through the $R$-factor minimization (Table I). When only the surface layer sites Ti1 and Ti2 (model 1–2) are included in the $R$-factor minimization, a high $R$ value of 0.774 is obtained. By accounting for the second layer sites Ti3 and Ti4 (model 1–4), the $R$ factor goes down very significantly by 0.222. More can be said by looking at the $R$ values obtained for single Ti emitters from Ti1 to Ti6 (line $R_n$ in Table I). The smallest (largest) value is obtained for Ti3 (Ti4) indicating that Ti3 (Ti4) carries the most (least) defect charge. Indeed in model 1–4, two-thirds of the weight are found on the Ti3 atom, while the contribution of Ti4 is negligible. Adding the third layer sites (model 1–6) reduces the $R$ factor by another 0.075, but this decrease is much less significant than that observed from model 1–2 to model 1–4. While the weight on the third layer atoms is rather high, the dominant contribution still comes from the Ti3 atoms.

We now turn to the PED patterns shown in Fig. 3, right-hand panels, which were calculated for the models 1–$n$ with the best-fit weights as given in Table I. The pattern 1–2 can roughly reproduce the experimental anisotropy in the region $\theta > 50°$, but it completely lacks the strong anisotropy observed in the central region ($\theta < 50$). This result immediately shows that a substantial part of the defect charge is located on subsurface layers. The patterns 1–4 and 1–6 both give satisfactory agreement with the experimental data. From a visual comparison, the quality of the fit is comparable for the two models, which is in line with the fact that the difference of the corresponding $R$ values is small. This means that the large weights of Ti5 and Ti6, obtained from the $R$-factor minimization in model 1–6, are not very significant and might well be overestimated.

Bridging oxygen vacancies have been identified as a major defect type of the reduced $TiO_2(110)$ surface in numerous scanning tunneling microscopy studies [1]. The role played by Ti interstitials is less clear. To shed some light on this issue, we have calculated the PED patterns from Ti interstitial sites closest to the surface, that is at the empty oxygen octahedra between the first and second TiO layer. There are two inequivalent sites: one (A) is at the midpoint between Ti1 and Ti3 and the other one (B) between Ti2 and Ti4. The calculated PED patterns

for these emitters (not shown) are very different from the experimental defect state PED pattern and give very high $R$ factors (0.944 for A and 1.001 for B). It is known from first-principles calculations that Ti interstitial atoms, if present, contribute substantially to the defect state [17]. Therefore our results provide evidence that Ti interstitial atoms are the minority defect type at the reduced $TiO_2(110)$ surface.

The above analysis leads to the following conclusions. The defect charge is distributed over several surface and subsurface lattice Ti sites. By far most of the charge is found on subsurface sites, with a maximum on the second layer site Ti3. The charge on the other second layer site (Ti4) is completely negligible. The surface layer sites, Ti1 and Ti2, carry a small, but non-negligible amount of charge. Note that the forward scattering analysis has led to qualitatively the same conclusions.

These findings agree well with DFT calculations, which predict a delocalization of the defect charge over several surface and subsurface Ti sites. According to Lindan *et al.* [4] the dominant contributions are located on Ti1 and Ti3 sites. However, our results are at odds with a more recent first-principles study by Di Valentin *et al.* [7] who used the B3LYP hybrid XC functional. These calculations predict that one of the two excess electrons is localized on a Ti1 site and the other one on a Ti2 site. The PED pattern calculated for such a defect charge distribution is very similar to 1–2 in Fig. 3. It can be discarded since it badly fits experiment and corresponds to a poor $R$ value of 0.787. Our experimental findings thus seem to contradict the theoretical results obtained within the B3LYP scheme, which is often found to provide a more accurate description of the electronic structure of oxides than DFT. One may speculate about the reasons for this apparent contradiction. The B3LYP calculations possibly give the correct ground state of the system, but the DFT picture describes better the electronic structure at room temperature, at which our experiments were carried out. This idea is based on the observation that some early transition metal oxides (e.g., $VO_2$) exhibit a phase transition between a low symmetry insulating (i.e., electron localized) phase at low temperature and a high symmetry metallic phase at high temperature. The B3LYP ground state of reduced $TiO_2(110)$ involves symmetry-breaking structural distortions which are a necessary condition for the localization of the defect charge on the sites Ti1 and Ti2 [7]. This implies that in a symmetry-restored high temperature phase the defect charge would be delocalized as predicted by DFT and as we have found here.

In summary we have shown that the defect charge of reduced $TiO_2(110)$ surfaces is shared by several surface and subsurface Ti sites in qualitative agreement with DFT calculations. The defect charge distribution is highly inhomogeneous with a dominant contribution on the subsurface site Ti3 and a negligible contribution on the subsurface site Ti4. More generally we have shown that the novel resonant photoelectron diffraction technique provides site and element specific information on the valence electronic structure of surfaces.


[1] U. Diebold, Surf. Sci. Rep. **48**, 53 (2003).
[2] Z. Zhang, S.-P. Jeng, and V. E. Henrich, Phys. Rev. B **43**, 12 004 (1991).
[3] P. Le Fèvre *et al.*, Phys. Rev. B **69**, 155421 (2004).
[4] P. J. D. Lindan, N. M. Harrison, M. J. Gillan, and J. A. White, Phys. Rev. B **55**, 15 919 (1997).
[5] A. T. Paxton and L. Thien-Nga, Phys. Rev. B **57**, 1579 (1998).
[6] T. Bredow and G. Pacchioni, Chem. Phys. Lett. **355**, 417 (2002).
[7] C. Di Valentin, G. Pacchioni, and A. Selloni, Phys. Rev. Lett. **97**, 166803 (2006).
[8] E. Serwicka, M. W. Schlierkamp, and R. N. Schindler, Z. Naturforsch. **36a**, 226 (1981).
[9] L. Floreano *et al.*, Rev. Sci. Instrum. **70**, 3855 (1999).
[10] M. Li *et al.*, Surf. Sci. **437**, 173 (1999).
[11] R. Lindsay *et al.*, Phys. Rev. Lett. **94**, 246102 (2005).
[12] The displacement along [110] of Ti2 relative to O2 is $-0.46 \pm 0.11$ Å according to Ref. [11].
[13] Yufeng Chen and Michel A. Van Hove (private communication).
[14] O. K. Andersen and O. Jepsen, Phys. Rev. Lett. **53**, 2571 (1984).
[15] The RP is an x-ray absorption $2p^6 3d^1 + \hbar\omega \rightarrow 2p^5 3d^2$ followed by the Auger-like decay $2p^5 3d^2 \rightarrow 2p^6 3d^0 + \epsilon_A l_A$, where $\epsilon_A l_A$ denotes an outgoing electron wave of energy $\epsilon_A$ and angular momentum $l_A$. The final state of the RP has the same electronic configuration as the DP $2p^6 3d^1 + \hbar\omega \rightarrow 2p^6 3d^0 + \epsilon_D l_D$, where, at resonance, $\epsilon_A = \epsilon_D$, but, in general, $l_A \neq l_D$. In the present case, the possible $l$ values are $l_D = 1, 3$ and $l_A = 1, 3, 5$, but in both processes the $l = 3$ channel strongly dominates. For the DP, this is due to the high energy behavior of the dipole matrix elements, and for Auger emission it was shown in [16].
[16] D. K. Saldin, G. R. Harp, and B. P. Tonner, Phys. Rev. B **45**, 9629 (1992).
[17] E. Cho *et al.*, Phys. Rev. B **73**, 193202 (2006).